IEEE Photonics Journal
An IEEE Photonics Society Publication

Open Access

High-Spatial- and Spectral-Resolution Time-Domain Brillouin Distributed Sensing by Use of Two Frequency-Shifted Optical Beam Pairs

Volume 4, Number 5, October 2012

A. Minardo
L. Zeni
R. Bernini

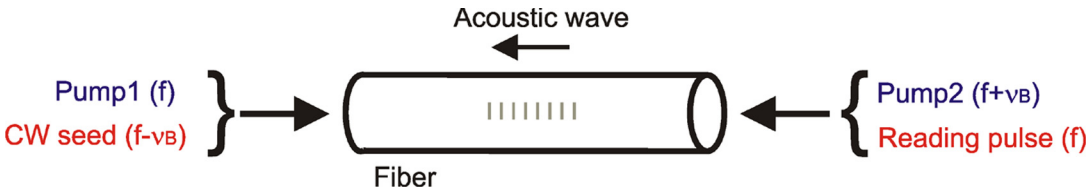

DOI: 10.1109/JPHOT.2012.2219301
1943-0655/$31.00 ©2012 IEEE

IEEE photonics SOCIETY

IEEE

High-Spatial- and Spectral-Resolution Time-Domain Brillouin Distributed Sensing by Use of Two Frequency-Shifted Optical Beam Pairs

A. Minardo,[1] **L. Zeni,**[1,2] **and R. Bernini**[2]

[1]Dipartimento di Ingegneria dell'Informazione, Seconda Università di Napoli, 81031 Aversa, Italy
[2]Istituto per il Rilevamento Elettromagnetico dell'Ambiente, Consiglio Nazionale delle Ricerche, 80124 Napoli, Italy

DOI: 10.1109/JPHOT.2012.2219301
1943-0655/$31.00 ©2012 IEEE

Manuscript received July 17, 2012; revised September 13, 2012; accepted September 13, 2012. Date of publication September 17, 2012; date of current version September 27, 2012. This work was supported in part by the European Community's Seventh Framework Program (FP7/2007–2013) under Grant Agreements 225663 and 265954 and in part by the European COST action TD1001-OFSESA. Corresponding author: A. Minardo (e-mail: aldo.minardo@unina2.it).

Abstract: We present a novel scheme aimed to improve spectral resolution in Brillouin distributed sensors based on single-mode standard fibers. The method makes use of two frequency-shifted optical pairs, the first one (the "writing" pair) devoted to excite the acoustic wave and the second one (the "reading" pair) employed to perform Brillouin gain interrogation. A numerical analysis demonstrates the capability of the method to ensure high spectral resolution even when operating in the high-spatial-resolution (~1 m or less) regime. Preliminary experimental results carried out at 1-m spatial resolution are also reported.

Index Terms: Brillouin fiber sensing, optical fiber measurement, stimulated Brillouin scattering (SBS).

1. Introduction

In distributed sensors based on the Brillouin optical time-domain analysis (BOTDA), an optical pulse interacts with a counterpropagating CW probe beam along an optical fiber, through an acoustic wave electrostrictively driven by the two optical beams. By recording the intensity of the emerging probe as a function of the time, the Brillouin gain is measured at each fiber position. As the same pump pulse is employed to generate the acoustic wave and sense it, reducing the pulse temporal width in the attempt to improve spatial resolution gives rise to a broader acoustic-wave spectrum [and therefore a broader and weaker Brillouin gain spectrum (BGS)], degrading the frequency resolution and the SNR of the sensor [1], [2]. In recent years, several techniques have been proposed to overcome this limitation. Most techniques rely on the separation between the process of acoustic-wave excitation and that of optical interrogation. For example, in methods based on Brillouin dynamic grating, the two aforementioned processes are separated by using a polarization-maintaining fiber as the sensing medium: the acoustic wave responsible for stimulated Brillouin scattering (SBS) is excited by two pumps polarized along one axis of the fiber, while optical reading is performed by injecting an orthogonally polarized pulsed beam [3]. In the differential pulsewidth pair method, the decoupling is performed numerically, by subtracting the Brillouin response acquired separately for two slightly different pulse durations [4]. In such a case, the common part of the pulse pair is devoted to acoustic-wave excitation, while the differential component performs the interrogation [5].

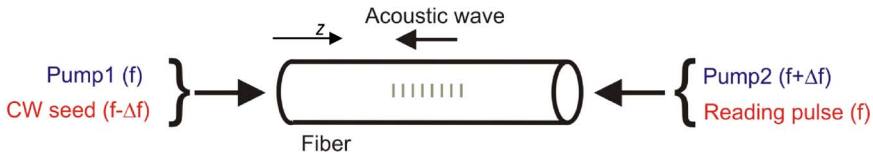

Fig. 1. Schematic of the dual optical beam pair scheme.

In this paper, we propose a novel method to separate the two processes, which can be applied to standard single-mode optical fibers. The method makes use of two optical beam pairs, each pair being composed of two frequency-shifted optical beams (see Fig. 1), and such that the optical beams associated to each pair are spectrally separated by the same quantity Δf. The first pair comprises two CW "writing" beams, indicated as pump1 and pump2 in Fig. 1, counterpropagating along the fiber. Provided that Δf is within the BGS of the fiber, these two pumps excite a stationary acoustic wave through electrostriction. The second optical pair (the "reading" pair) is composed of a CW optical seed beam and an optical "reading" pulse, with the latter having the same carrier frequency of pump1. The reading pulse is employed for the readout of the acoustic wave excited by the two pumps, while it will be shown later that the beam at frequency $f - \Delta f$ acts as a seed to enhance the magnitude of the Brillouin scatter signal.

The proposed interrogation scheme is aimed to perform distributed sensing at high spatial resolution (as determined by the duration of the reading pulse) while keeping a narrow BGS (i.e., high spectral resolution). In particular, in absence of a seed beam, the acoustic wave will be uniquely generated by the two writing pumps. The excited acoustic wave will scatter the optical reading pulse, producing a back reflected signal at frequency $f - \Delta f$. As the scattering source is a stationary acoustic wave, the BGS will keep its natural linewidth, independently of the duration of the optical reading pulse [3]. However, as it will be shown numerically, in this condition, the Brillouin gain is very low. By injecting at $z = 0$ (leftmost end of the fiber) a seed beam at frequency $f - \Delta f$, the magnitude of the signal at the same frequency $(f - \Delta f)$ detected at $z = L$ (rightmost end of the fiber) will be strongly enhanced. However, we also observe that the injected seed interacts with the reading pulse, generating an acoustic wave at the same frequency (Δf) of the stationary acoustic wave excited by the writing pair. As this second contribution is generated by a short optical pulse, it will be broadband [2]. If the magnitude of the broadband acoustic wave is comparable with that of the stationary one, the observed BGS will broaden with consequent loss of spectral resolution. In the next section, we demonstrate that, by properly tuning the input powers of the various optical beams involved, a compromise can be found between magnitude of the Brillouin signal and BGS bandwidth.

2. Numerical Analysis

In this section, we report the results of a numerical analysis aimed to assess the effectiveness of the proposed method. Numerical tests were carried out by solving the following set of five scalar-coupled wave equations [6]:

$$\left(-\frac{\partial}{\partial z}+\frac{1}{v_g}\frac{\partial}{\partial t}\right)E_{p1} = -QE_{p2} \tag{1a}$$

$$\left(\frac{\partial}{\partial z}+\frac{1}{v_g}\frac{\partial}{\partial t}\right)E_{p2} = Q^*E_{p1} \tag{1b}$$

$$\left(-\frac{\partial}{\partial z}+\frac{1}{v_g}\frac{\partial}{\partial t}\right)E_{s} = Q^*E_{r} \tag{1c}$$

$$\left(\frac{\partial}{\partial z}+\frac{1}{v_g}\frac{\partial}{\partial t}\right)E_{r} = -Q^*E_{s} \tag{1d}$$

$$\left(\frac{\partial}{\partial t}+\Gamma\right)Q = \frac{1}{2}\Gamma_1 g_B\left(E_{p1}E_{p2}^* + E_sE_r^*\right). \tag{1e}$$

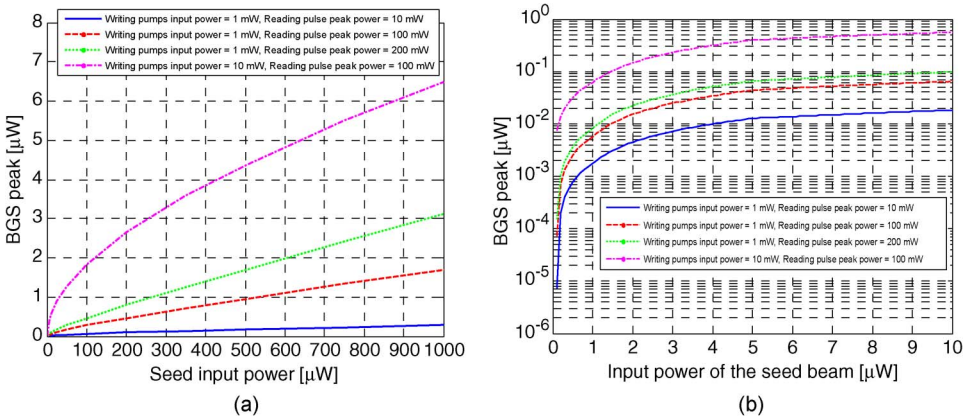

Fig. 2. BGS peak computed for a 5-m uniform fiber represented in a linear scale (a) or a semilogarithmic scale for a reduced range of the seed input power (b).

Here, E_{p1}, E_{p2}, E_s, E_r, and Q stand for the complex amplitudes of pump1 (at frequency f), pump2 (at frequency $f + \Delta f$), the seed beam, the reading pulse, and the acoustic field, respectively. g_B is the SBS gain coefficient, v_g is the optical group velocity, $\Gamma = \Gamma_1 + j\Delta$, where $\Gamma_1 = 1/(2\tau)$ ($\tau \approx 6$ ns is the phonon lifetime for silica fibers) is the damping rate, and $\Delta(z) = 2\pi(\Delta f - \nu_B(z))$ is the z-dependent detuning frequency, i.e., the difference between the frequency shift of the beams composing each pair (Δf) and the local Brillouin frequency (ν_B). Note from (1e) that the acoustic wave is driven by two sources, the first one associated to the writing pumps and the second one associated to the reading pair. Finally, the constant fiber loss has been omitted.

The boundary conditions for (1) are $E_{P1}(0, t) = E_{p10}$, $E_{P2}(L, t) = E_{p2L}$, $E_S(0, t) = E_{s0}$, and $E_r(L, t) = E_r(t)$, where $E_r(t)$ represents the waveform of the interrogation pulse at its input section. Eqs. (1) were solved by the Leveque wave propagation method [7], based on the time updating of the initial solution resulting from the SBS stationary equations. Numerical tests were performed for a Brillouin gain $g_B = 1.44 \cdot 10^{-11}$ m/W, a damping factor $\Gamma_1 = \pi \times 35$ MHz, and a duration of the optical reading pulse equal to 5 ns.

The first numerical tests were performed for a uniform 5-m-long fiber. For each test case, we computed the intensity of the seed beam transmitted at $z = L$ as a function of time since the instant of launch of the reading pulse, while varying the detuning frequency from 0 MHz to 75 MHz. As in conventional BOTDA, each time instant is associated to a specific position along the fiber through the time of flight of the pulse. The computed traces were employed to extract the BGS (i.e., the amplification of the transmitted seed beam) at each fiber position. We report in Fig. 2 the BGS peak computed at the fiber mid section $(z = 2.5$ m$)$ for each test case.

The input power of the seed beam was varied between 0 and 1000 μW. Also, the input power of the writing pumps was set to either 1 mW or 10 mW, while the reading pulse peak power was set to 10 mW, 100 mW, or 200 mW. Fig. 2(a) shows that the magnitude of the Brillouin signal increases with the intensity of the injected seed. It is important to underline that the BGS peak calculated in absence of seed beam (i.e., by solving (1) for $E_S(0, t) = 0$) is not zero as it may appear from Fig. 2(a); rather, it reaches a very low value. To better illustrate this point, we report in Fig. 2(b) the BGS peak in a semilogarithm scale and for a reduced range of the seed input power. For example, for an input power of the writing pumps equal to 1 mW and a peak power of the reading pulse equal to 10 mW (blue line), the BGS peak calculated in absence of an injected seed beam is $\sim$7 pW. Such a value increases to $\sim$60 nW for an input seed power as low as 100 μW. Fig. 2(a) also shows that the magnitude of the Brillouin gain increases with the input power of the writing pumps and the power of the reading pulse. However, we must also take into account the effect of these parameters on the BGS bandwidth. The full-width-at-half-maximum (FWHM) BGS bandwidth is reported in Fig. 3, which shows that, for each fixed input power of the writing pumps, the bandwidth increases with the power of the reading pulse and that of the seed beam.

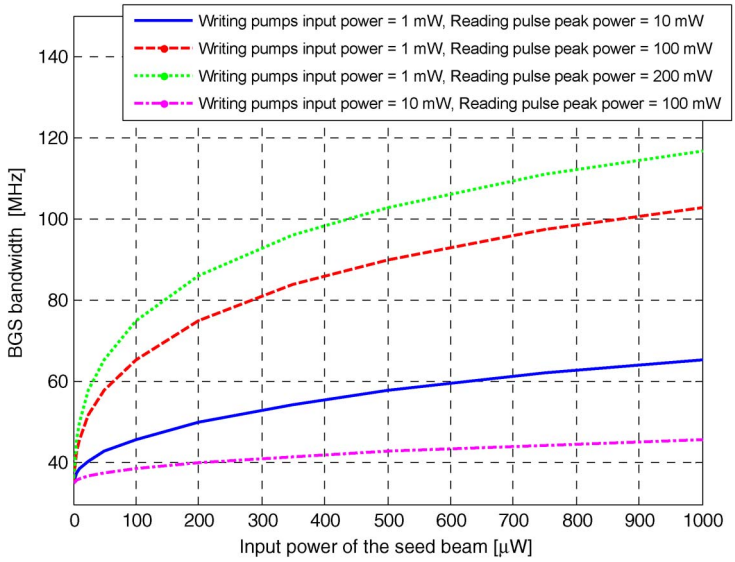

Fig. 3. BGS bandwidth computed for a 5-m uniform fiber.

As discussed earlier, this effect is related to the broadband acoustic wave generated by the reading pair. Fig. 3 shows that this effect can be counteracted by increasing the power of the writing pumps. For example, for an input power of the writing pumps equal to 10 mW, the BGS bandwidth is lower than 45 MHz within the whole range of reading pair powers set in the simulation. Still, this can be explained by considering that the observed BGS is the sum of a narrowband contribution associated to the writing pair and a broadband contribution associated to the reading pair [see (1e)]. Figs. 2 and 3 demonstrate that a compromise between BGS peak and BGS bandwidth can be found, by properly setting the input powers of the various optical beams involved. We finally note that, for a reading pulse shorter than 5 ns, the resulting BGS bandwidth will be larger than that reported in Fig. 3 for any set of input optical powers. Therefore, a reduced power of the reading optical pair or an increased power of the writing optical pair should be employed in case of shorter pulses in order to ensure the same FWHM bandwidths reported in Fig. 3.

Next simulations were done by considering a 5-m-long fiber including a 50-MHz perturbation in the Brillouin shift extending from $z = 2.5$ m to $z = 3.5$ m. In this case, the input power of the writing pumps was set to 10 mW, the peak power of the reading pulse was set to 100 mW, and the input power of the seed beam was set to 1 mW. In Fig. 4(a), we report the calculated Brillouin gain versus location and frequency. It is seen that the sensor is able to detect accurately the perturbation.

In order to best appreciate the response of the sensor, we report in Fig. 4(b) the Brillouin gain computed along the fiber in case of optical pairs resonant either at the perturbation or outside the perturbation. The rise and fall times of the traces ($\sim$5 ns) confirm that the sensor exhibits a 50-cm spatial resolution, as determined by the duration of the reading pulse.

Fig. 5(a) reports the BGS at two fiber sections: the first one taken immediately before the perturbation (at $z = 2$ m) and the second one taken along the perturbation (at $z = 3.3$ m). Both spectra exhibit a FWHM bandwidth of $\sim$43 MHz, in agreement with the calculations performed for a uniform fiber (see Fig. 3). Moreover, the spectrum calculated at $z = 3.3$ m has no residual peak associated to the background fiber. For comparison purposes, we also report in Fig. 5(a) the BGS at the same fiber section, computed for a standard BOTDA configuration and equivalent pulse parameters. The corresponding BGS bandwidth is 186 MHz. Therefore, applying the proposed method the same spatial resolution can be achieved with an about fourfold BGS narrowing. The above simulations were carried out by supposing a reading pulse with no pedestal. In real cases, the finite extinction ratio (ER) of the modulator employed to form the pulses results in a reading pulse composed of a pulsed component, superimposed to a finite pedestal. In order to evaluate the effect of the pulse baseline on the signals acquired with the proposed configuration, we performed a

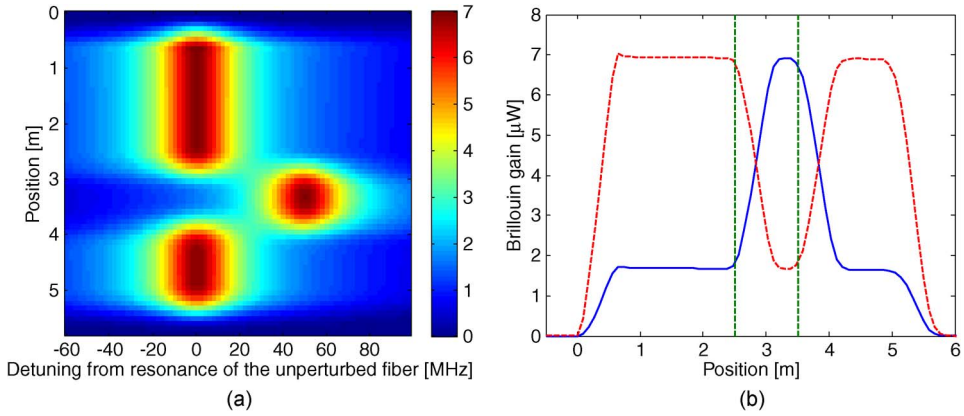

Fig. 4. (a) Brillouin gain distribution calculated for a 5 m-long fiber with a 1 m-long, 50 MHz perturbation in the middle. The reading pulse is 5 ns long and has no baseline. Colorbar values are in μW. (b) Brillouin gain at zero detuning (solid blue line) and at 50 MHz detuning (red dashed line). The vertical dashed lines indicate the perturbed region.

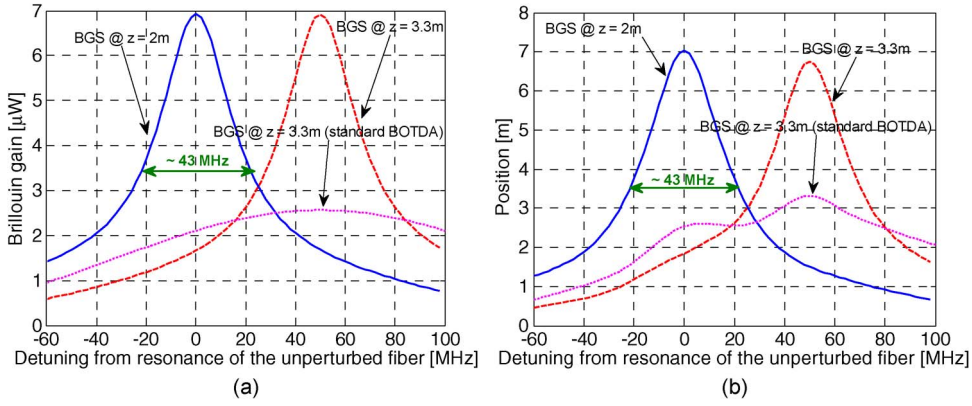

Fig. 5. BGS computed at $z = 2$ m (blue solid line) and $z = 3.3$ m (red dashed line) for our method, and BGS computed at $z = 3.3$ m for a standard BOTDA configuration (magenta dotted line), in case of (a) no pulse pedestal or (b) ER $= 20$ dB.

new simulation by keeping the same parameters as above, with the only difference being the addition of a -20 dB (1 mW) baseline to the reading pulse. Therefore, the system represented by (1) was solved by imposing as boundary condition $E_r(L, t) = E_r(t) + E_r0$, in which Er(t) is the 5-ns pulse and E_r0 is the pulse pedestal. The computed Brillouin gain spectra at the same positions as before are reported in Fig. 5(b). The figure shows that the addition of a relatively large pedestal to the pulse does not influence significantly the response of the sensor in our configuration. On the other hand, the BGS computed at $z = 3.3$ m for a standard BOTDA scheme and identical pump pulse characteristics (duration of 5 ns and ER $= 20$ dB), also shown in Fig. 5(b), exhibits a significant residual peak centered at zero detuning, arising from the interaction between the pulse baseline and the decaying acoustic wave excited by the pulse at adjacent points in the fiber [8], [9].

In our configuration and with the optical powers chosen for this simulation, the Brillouin signal is mainly due to the scattering of the reading pulse with the stationary acoustic wave formed by the writing pair; therefore, any spurious effect related to the decaying acoustic wave (i.e., the one excited by the reading pulse in the fiber positions preceding the perturbation) is much attenuated.

In conclusion, the numerical analysis demonstrates that the proposed configuration allows to achieve a Brillouin response possessing simultaneously high spatial and spectrum resolution. Also, the distorting effects associated to the pulse leakage in the standard BOTDA method are attenuated.

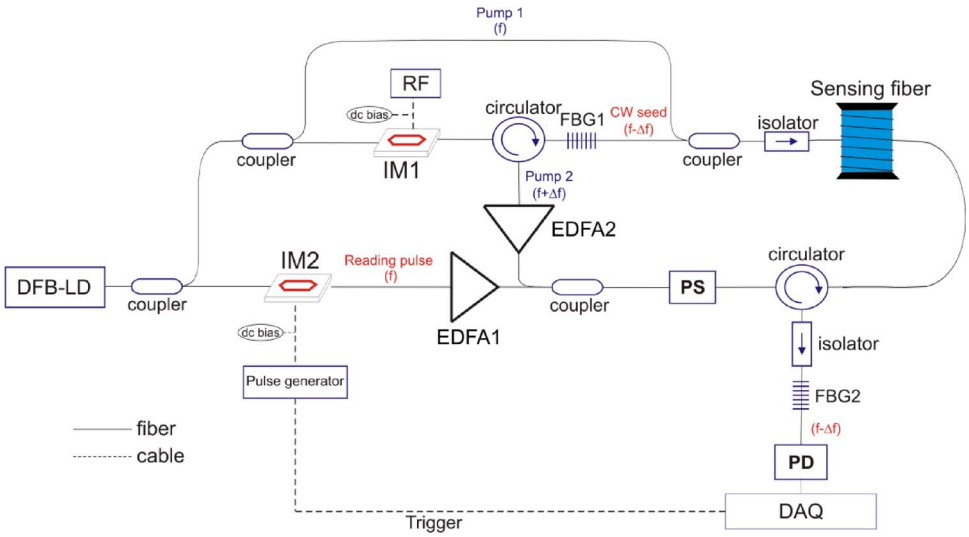

Fig. 6. Experimental setup for Brillouin measurements based on a dual optical beam pair pumping scheme. IM: intensity modulator; EDFA: erbium-doped fiber amplifier; FBG: fiber Bragg grating; PS: polarization scrambler; PD: photodetector.

3. Experimental Results

A number of preliminary experimental tests have been carried out by use of the setup shown in Fig. 6 schematically. In order to ensure stability, the optical beams were all derived from the same distributed-feedback laser diode (DFB-LD), emitting at 1550.12 nm. The laser light was first split in two branches by use of a 3-dB coupler, with the lower branch employed to form the reading pulses and the upper one devoted to the remaining beams. The reading pulse was generated by the intensity modulator IM2 connected to an electrical pulse generator and properly biased in order to minimize the pulse pedestal.

The light in the upper branch was further split by another 3-dB coupler, so that half of the power was directly employed as pump1 (at the laser frequency), while the other half was employed to generate pump2 and the seed. In particular, by driving the intensity modulator IM1 by a microwave sweeper and a dc bias adjusted in order to operate in the suppressed carrier regime, the frequency-downshifted seed beam and the frequency-upshifted pump2 were generated at the exit of IM1. An optical circulator and the narrowband fiber Bragg grating FBG1 were employed to separate the two sidebands exiting from IM1. Just before the photodetector PD, another optical filter (FBG2) was used to filter out pump1 and select the seed beam. If not properly filtered, pump1 may lead to increased noise and a saturation at the photodetector PD, hindering the amplification of the received seed beam. The two optical filters were nominally identical, with a 3-dB reflection bandwidth of 5 GHz and a peak reflectivity of 99%. A polarization scrambler (PS) was used to scramble the state of polarization (SOP) of both the reading pulse and pump2, so as to average out the polarization-sensitive Brillouin gain. The photodetector PD had a bandwidth of 125 MHz and a transimpedence gain of 40.000 V/W, while the acquisition card had a bandwidth of 300 MHz and a sampling rate of 1 GS/s.

The first experimental test was performed on a 33-m-long single-mode fiber sample having a nominal Brillouin frequency shift of 10885 MHz, along which two fiber strands with a Brillouin frequency shift of 10670 MHz were inserted by fusion splicing. The first strand was inserted between $z = 22.3$ m and $z = 24$ m, while the second one was placed between $z = 29.6$ m and $z = 31.2$ m.

The reading pulse had a duration of 10 ns (as dictated by the minimum duration of the pulses provided by the electrical pulse generator) and an ER of ~ -30 dB. The power of the optical beams at the entrance of the sensing fiber was $\sim$1 mW for both pump1 and the CW seed. The peak power of the pulse exiting from EDFA1 was $\sim$500 mW, while the power of pump2 was varied by adjusting the optical gain of EDFA2. In this way, we could modify the intensity of the stationary acoustic wave

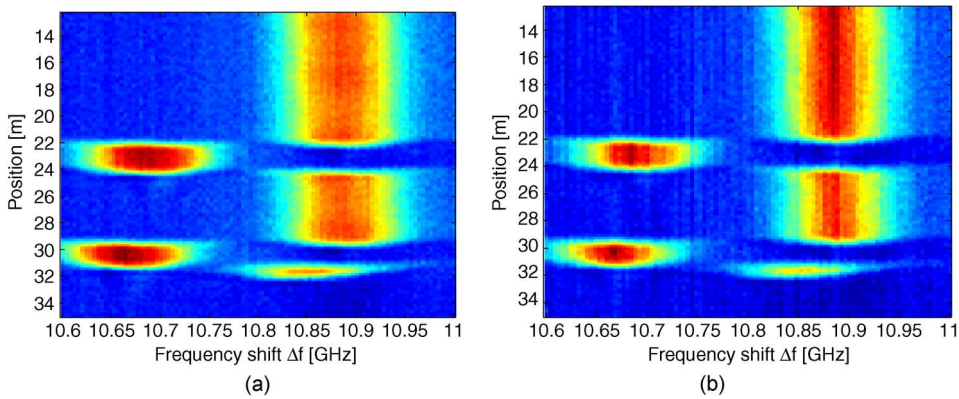

Fig. 7. BGS map versus frequency shift and position, measured by using the dual optical beam pairs method along a 33-m fiber sample, for (a) Pp2 = 0; (b) = Pp2 = 40 mW.

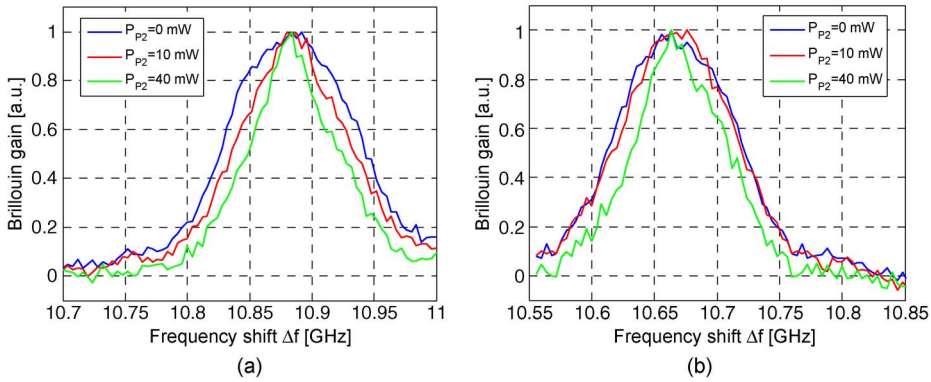

Fig. 8. BGSs measured by using the dual optical beam pairs method at $z = 1.2$ m (a) and 31 m (b) of a 35-m long fiber sample, for three different input powers of the second pump.

produced by the writing pair by properly adjusting the EDFA2 gain. We compare in Fig. 7 the BGS distribution along the last 20 m as measured for an input power of pump2 equal to 0 mW (i.e., by physically disconnecting the output of EDFA2 from the coupler input), and an input power of pump2 equal to 40 mW. Note that, in the former case, no stationary acoustic wave was excited; therefore, the results are expected to be equivalent to a standard BOTDA configuration.

A narrowing of the BGS at each fiber position can be observed by use of the proposed method. To better illustrate this point, we report in Fig. 8 the BGS at two fiber sections, the first one taken along the unperturbed fiber $(z = 1.2\ \text{m})$ and the second one taken along the second spliced segment $(z = 31\ \text{m})$, for three different input powers of pump2 (0, 10, and 40 mW). Both spectra indicate that the bandwidth decreases by increasing the power of the writing pump. In particular, the FWHM bandwidths of the BGS reported in Fig. 8(a) were 117 MHz, 98 MHz, and 74 MHz for the three considered pump2 powers, respectively.

The narrowing of the BGS for an increasing power of one of the two writing pumps is coherent with the numerical analysis presented previously. Actually, we repeated the calculation of the BGS bandwidth by use of (1) after setting the parameters as in our experimental conditions, while varying the input power of pump2 from 0 mW to 200 mW (see Fig. 9). The calculated BGS bandwidths for the input pump2 power used in the experiments were 113 MHz, 97 MHz, and 76 MHz, respectively. Therefore, a good agreement was found between the numerical and experimental bandwidths.

Although a reduction of the BGS bandwidth of ~35% was achieved by the proposed method, it was not possible to reduce further the BGS bandwidth by increasing the power of pump2, due to

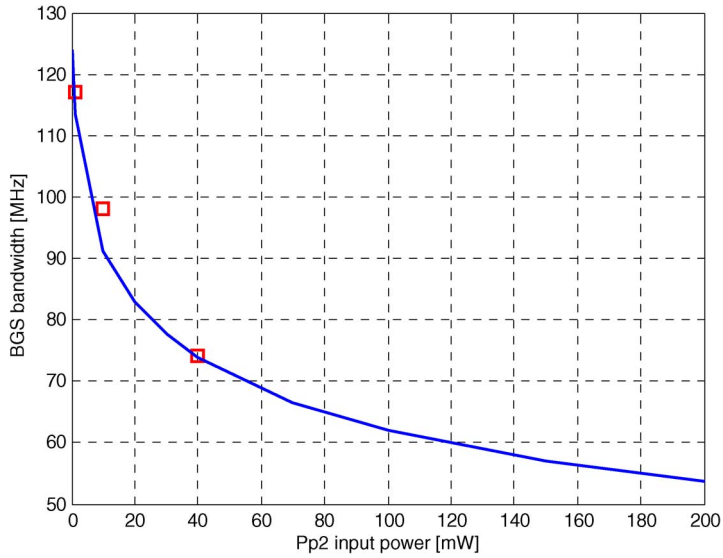

Fig. 9. BGS bandwidth computed for the experimental conditions of Fig. 7, as a function of the input power of Pp2. The red squares indicate the experimental values.

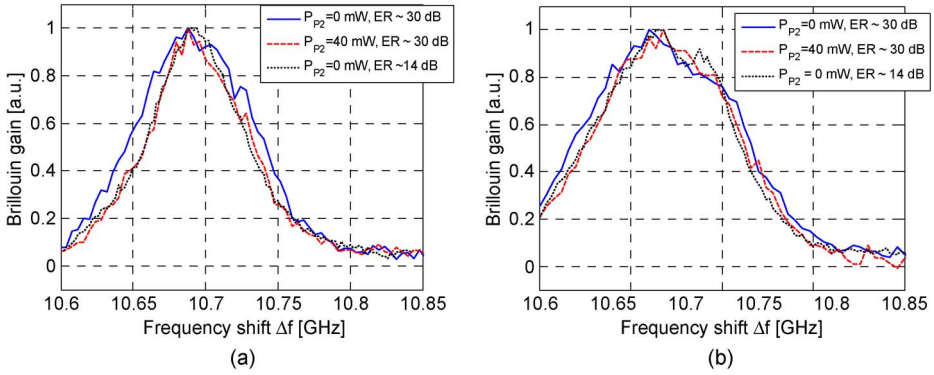

Fig. 10. Normalized BGS measured by using the proposed method at $z = 2$ m (a) and 5 m (b) of a 6-m fiber sample, or by using the standard BOTDA for two different baseline levels for the reading pulse.

EDFA2 output power saturation. On the other hand, the BGS bandwidth may be also reduced by increasing the power of pump1. However, increasing the power of pump1 also leads to a larger noise in the retrieved spectra, due to the interference between two counterpropagating optical beams (pump1 and reading pulse) having the same carrier frequency [10]. Therefore, pump1 must be kept at a sufficiently low power.

As discussed in the numerical section, the BGS can be narrowed also by reducing the power of the reading pulse and/or of the seed beam. However, this also leads to a weaker Brillouin gain and thus to a poorer SNR.

Further experiments were performed on a 6-m-long fiber sample comprised of two strands having a close Brillouin frequency shift. In particular, the fiber was composed of a first strand with a nominal Brillouin shift of ≈10690 MHz (from $z = 0$ to $z = 4$ m) and a second strand with a nominal Brillouin shift of ≈10670 MHz (from $z = 4$ m to $z = 6$ m). We report in Fig. 10 the BGS at two sections ($z = 2$ m and $z = 5$ m), acquired in absence or in presence $(\text{Pp2} = 40\ \text{mW})$ of pump2. The measurement for Pp2 = 0 mW was also repeated after increasing the pump baseline, by properly adjusting the dc bias voltage applied to IM2. In particular, the pulse ER was set to ∼14 dB, so as to achieve a BGS bandwidth as close as possible to the value observed for our method with

Pp2 = 40 mW (∼75 MHz). Comparing the spectra in Fig. 10(b), we see that, although the BGS bandwidth can be narrowed in the standard BOTDA configuration by simply increasing the pulse baseline, this solution also enhances the Brillouin residual peak at ∼10690 MHz, due to the interaction between the pulse baseline and the transient acoustic wave excited by the pulse along the first fiber strand.

Therefore, in the BOTDA method, the higher spectral resolution allowed by a large pulse pedestal comes at the price of a reduced spectral purity [8], [9], [11]. On the other hand, applying the proposed method the BGS narrowing is achieved without incurring in a loss of spectral purity, as it is deduced from Fig. 10(b) and from the numerical results shown in the previous section.

4. Conclusion

A new technique aimed to retrieve the Brillouin shift distribution along an optical fiber with high spatial and spectral resolution was proposed and demonstrated. The method utilizes two optical beam pairs, each one composed of two counterpropagating frequency-shifted optical beams. The stationary acoustic wave excited by the first optical pair enhances the SBS interaction between the beams of the second pair in a narrow spectral region around the Brillouin resonance, allowing to obtain high spectral resolution even when adopting a short interrogating pulse duration. Compared with a standard BOTDA configuration, the added complexity of the proposed setup is relatively modest. On the other side, the simultaneous propagation of two counterpropagating optical beams at the same frequency gives rise to added noise due to coherent Rayleigh scattering [10]. This problem may be circumvented by using two optical pairs spectrally separated by a quantity larger than the Brillouin shift (i.e., with pump1 at a carrier frequency different from that of the reading pulse), so that all the four optical beam involved would have a different carrier frequency. Note that the Brillouin shift is only slightly dependent on the pump carrier frequency (about 600-kHz variation for a pump optical frequency change of 10 GHz [12]); therefore, the technique may still be applied using two optical pairs shifted by a few tens of GHz each other.

References

[1] A. Fellay, L. Thévenaz, L. Facchini, M. Nikles, and M. Robert, "Distributed sensing using stimulated Brillouin scattering: Towards ultimate resolution," in *Proc. 12th Int. Conf. Opt. Fiber Sens. Tech. Dig.*, 1997, pp. 324–327.
[2] A. Minardo, R. Bernini, and L. Zeni, "Stimulated Brillouin scattering modeling for high-resolution, time-domain distributed sensing," *Opt. Exp.*, vol. 15, no. 16, pp. 10 397–10 407, Aug. 2007.
[3] K. Y. Song, W. Zou, Z. He, and K. Hotate, "Optical time-domain measurement of Brillouin dynamic grating spectrum in a polarization-maintaining fiber," *Opt. Lett.*, vol. 34, no. 9, pp. 1381–1383, May 2009.
[4] W. Li, X. Bao, Y. Li, and L. Chen, "Differential pulse-width pair BOTDA for high spatial resolution sensing," *Opt. Exp.*, vol. 16, no. 26, pp. 21 616–21 625, Dec. 2008.
[5] A. Minardo, R. Bernini, and L. Zeni, "Differential techniques for high-resolution BOTDA: An analytical approach," *IEEE Photon. Technol. Lett.*, vol. 24, no. 15, pp. 1295–1297, Aug. 2012.
[6] V. Lecoeuche, D. J. Webb, C. N. Pannell, and D. A. Jackson, "Transient response in high-resolution Brillouin-based distributed sensing using probe pulses shorter than the acoustic relaxation time," *Opt. Lett.*, vol. 25, no. 3, pp. 156–158, Feb. 2000.
[7] R. J. LeVeque, "Wave propagation method algorithms for multi-dimensional hyperbolic systems," *J. Comput. Phys.*, vol. 131, no. 2, pp. 327–353, Mar. 1997.
[8] A. Minardo, R. Bernini, and L. Zeni, "Numerical analysis of single pulse and differential pulse-width pair BOTDA systems in the high spatial resolution regime," *Opt. Exp.*, vol. 19, no. 20, pp. 19 233–19 244, Sep. 2011.
[9] J.-C. Beugnot, M. Tur, S. F. Mafang, and L. Thévenaz, "Distributed Brillouin sensing with sub-meter spatial resolution: Modeling and processing," *Opt. Exp.*, vol. 19, no. 8, pp. 7381–7397, Apr. 2011.
[10] K. De Souza, "Significance of coherent Rayleigh noise in fibre-optic distributed temperature sensing based on spontaneous Brillouin scattering," *Meas. Sci. Technol.*, vol. 17, no. 5, pp. 1065–1069, May 2006.
[11] A. Minardo, R. Bernini, and L. Zeni, "Spatial resolution enhancement in pre-activated BOTDA schemes by numerical processing," *IEEE Photon. Technol. Lett.*, vol. 24, no. 12, pp. 1003–1005, Jun. 2012.
[12] A. Zornoza, D. Olier, M. Sagues, and A. Loayssa, "Brillouin spectral scanning using the wavelength dependence of the frequency shift," *IEEE Sensors J.*, vol. 11, no. 2, pp. 382–383, Feb. 2011.